Dynamic control of refractive index during pulsed-laser-deposited waveguide growth

JAMES A. GRANT-JACOB,[1,*] STEPHEN J. BEECHER,[1] HARIS RIRIS,[2] ANTHONY W. YU,[2] DAVID P. SHEPHERD,[1] ROBERT W. EASON[1] AND JACOB I. MACKENZIE[1]

[1]*Optoelectronics Research Centre, University of Southampton, Highfield, Southampton SO17 1BJ, UK*
[2]*Laser & Electro-Optics Branch, NASA Goddard Space Flight Center, Greenbelt, Maryland 20771, USA*
** J.A.Grant-Jacob@soton.ac.uk*

Abstract: Engineering the optical properties of waveguides is important for optimization of their guided optical mode characteristics. Here, we document dynamic control of the refractive index and composition of crystalline films, via the substrate temperature, during pulsed-laser-deposition growth of Er(1%)-doped yttrium gallium garnet on <100>-orientated single-crystal yttrium aluminium garnet. An increasing substrate temperature is observed to reduce the gallium content in the grown film, with a corresponding reduction of refractive index. We demonstrate the ability to accurately control the refractive index via this technique and use it to grow a complex multi-core crystal waveguide. Our results highlight the potential of using pulsed laser deposition to fabricate crystal films with bespoke optical properties and thus engineer passive and active waveguide devices in situ.

OCIS codes: (310.0310) Thin films; (310.1860) Deposition and fabrication; (310.4165) Multilayer design; (230.7390) Waveguides, planar; (220.0220) Optical design and fabrication.

References and links

1. Q. Wu, J. P. Turpin, and D. H. Werner, "Integrated photonic systems based on transformation optics enabled gradient index devices," Light Sci Appl **1**, e38 (2012).
2. Z. Wang, X. Xu, D. Fan, Y. Wang, H. Subbaraman, and R. T. Chen, "Geometrical tuning art for entirely subwavelength grating waveguide based integrated photonics circuits," Sci. Rep. **6**, 24106 (2016).
3. D. S. Gill, A. A. Anderson, R. W. Eason, T. J. Warburton, and D. P. Shepherd, "Laser operation of an Nd:$Gd_3Ga_5O_{12}$ thin-film optical waveguide fabricated by pulsed laser deposition," Appl. Phys. Lett. **69**, 10–12 (1996).
4. A. A. Anderson, R. W. Eason, L. M. B. Hickey, M. Jelinek, C. Grivas, D. S. Gill, and N. A. Vainos, "Ti:sapphire planar waveguide laser grown by pulsed laser deposition," Opt. Lett. **22**, 1556–1558 (1997).
5. A. Zakery, Y. Ruan, A. V. Rode, M. Samoc, and B. Luther-Davies, "Low-loss waveguides in ultrafast laser-deposited As_2S_3 chalcogenide films," J. Opt. Sci. Am. B, Vol. **20pp**, 1844–1852 (2003).
6. S. J. Beecher, T. L. Parsonage, J. I. Mackenzie, K. A. Sloyan, J. A. Grant-Jacob, and R. W. Eason, "Diode-end-pumped 1.2 W Yb:Y_2O_3 planar waveguide laser," Opt. Express **22**, 22056 (2014).
7. J. A. Grant-Jacob, S. J. Beecher, T. L. Parsonage, P. Hua, J. I. Mackenzie, D. P. Shepherd, and R. W. Eason, "An 11.5 W Yb:YAG planar waveguide laser fabricated via pulsed laser deposition," Opt. Mater. Express **6**, 91–96 (2016).
8. J. Lancok, M. Jelinek, and F. Flory, "Optical properties of PLD-created Nd:YAG and Nd:YAP planar waveguide thin films," in P. A. Atanasov and D. V. Stoyanov, eds. (SPIE, 1999), Vol. 3571, p. 364.
9. T. C. May-Smith, C. Grivas, D. P. Shepherd, R. W. Eason, and M. J. F. Healy, "Thick film growth of high optical quality low loss (0.1dBcm^{-1}) Nd:$Gd_3Ga_5O_{12}$ on $Y_3Al_5O_{12}$ by pulsed laser deposition," Appl. Surf. Sci. **223**, 361–371 (2004).
10. J. A. Grant-Jacob, S. J. Beecher, T. L. Parsonage, P. Hua, J. I. Mackenzie, D. P. Shepherd, and R. W. Eason, "Engineering of thin crystal layers grown by pulsed laser deposition," in *Proc. SPIE 9893, Laser Sources and Applications III*, J. I. Mackenzie, H. Jelínková, T. Taira, and M. Abdou Ahmed, eds. (SPIE, 2016), Vol. 9893, p. 98930E.
11. J. I. Mackenzie, J. A. Grant-Jacob, S. Beecher, H. Riris, A. W. Yu, D. P. Shepherd, and R. W. Eason, "Er:YGG planar waveguides grown by pulsed laser deposition for LIDAR applications," in *Proc. SPIE, Solid State Lasers XXVI: Technology and Devices*, W. A. Clarkson and R.K. Shori, eds. (SPIE, 2017), Vol. 10082, p. 100820A–10082–7.

12. T. Sakimura, Y. Watanabe, T. Ando, S. Kameyama, K. Asaka, H. Tanaka, T. Yanagisawa, Y. Hirano, and H. Inokuchi, "3.2 mJ, 1.5 μm laser power amplifier using an Er, Yb: glass planar waveguide for a coherent Doppler LIDAR," in *Proceedings of 17th Coherent Laser Radar Conference* (2013).
13. H. Riris, K. Numata, S. Li, S. Wu, A. Ramanathan, M. Dawsey, J. Mao, R. Kawa, and J. B. Abshire, "Airborne measurements of atmospheric methane column abundance using a pulsed integrated-path differential absorption lidar," Appl. Opt. **51**, 8296–8305 (2012).
14. R. W. Eason, T. C. May-Smith, C. Grivas, M. S. B. Darby, D. P. Shepherd, and R. Gazia, "Current state-of-the-art of pulsed laser deposition of optical waveguide structures: Existing capabilities and future trends," Appl. Surf. Sci. **255**, 5199–5205 (2009).
15. T. C. May-Smith, A. C. Muir, M. S. B. Darby, and R. W. Eason, "Design and performance of a ZnSe tetra-prism for homogeneous substrate heating using a CO_2 laser for pulsed laser deposition experiments," Appl. Opt. **47**, 1767 (2008).
16. A. Sposito, "Pulsed laser deposition of thin film magneto-optic materials and lasing waveguides," Ph.D. thesis, University of Southampton (2014).
17. 23848, "Inorganic Crystal Structure Database (ICSD)," http://icsd.cds.rsc.org.
18. 14343, "Inorganic Crystal Structure Database (ICSD)," http://icsd.cds.rsc.org.
19. 82420, "Inorganic Crystal Structure Database (ICSD)," http://icsd.cds.rsc.org.
20. 39186, "Inorganic Crystal Structure Database (ICSD)," http://icsd.cds.rsc.org.
21. Y. Nigara, "Measurement of the Optical Constants of Yttrium Oxide," Jpn. J. Appl. Phys. **7**, 404 (1968).
22. K. Enke and W. Tolksdorf, "Continuously recording refractive index spectrograph for transparent and opaque insulators and semiconductors," Rev. Sci. Instrum. **49**, 1625–1628 (1978).
23. P. Hertel, *Continuum Physics*, Graduate Texts in Physics (Springer Berlin Heidelberg, 2012).

1. Introduction

The ability to tailor the properties of a given material to optimize its end application is a universal goal within the manufacturing and materials development community. In the field of optics and photonics for example, properties such as the optical transmission or absorption, refractive index, material dispersion or ability to incorporate dopants are all examples where material design and engineering play a key role, and there are ready examples in components such as optical fibres, liquid crystal devices and integrated optical systems.

In the field of thin-films and optical waveguides, the refractive index of the guide relative to that of the substrate is of critical importance to ensure optimum control of the light confinement within the guiding structure, which in turn influences the optical loss, the mode structure, the polarization state, the propagation velocity and many other parameters of a particular design. To be able to engineer the refractive index profile within an optical waveguide takes this one step further as structures that have stepped, graded, or even Gaussian profiles find immediate application in a wide range of integrated optical waveguide applications [1,2]. This level of control can be accomplished in materials such as glasses and crystals by specific post-processing techniques such as in-diffusion or directly written by exposure to light or particle (ion or electron) bombardment. However, the ability to permanently modify the optical properties of a crystalline host material such as yttrium aluminium garnet (YAG) or $LiNbO_3$ *during* growth is far less readily accomplished to produce, for example, a gradient profile of the refractive index within the 1-10 μm depth of a typical guide.

Pulsed laser deposition (PLD) is a method for fabricating such optical films by using high-energy laser pulses to transfer material from a target to a substrate via an ablation plume [3–7]. To date, single-crystal garnet films have been grown via PLD to produce low-loss planar waveguides from target materials that include single crystals and sintered ceramics [8,9]. Furthermore, the PLD technique has been shown to be a versatile and relatively simple method to produce designer or bespoke compositions and hence material properties. In practice these properties are determined by the growth conditions that involve the four basic control parameters of target composition, ablation laser pulse energy and fluence on target, the background gas and the substrate temperature, and all these affect the stoichiometry, degree of crystallinity and refractive index of the film produced [10].

In this paper we show that by systematically varying the substrate temperature during PLD, bespoke waveguides with complex refractive index profiles, such as those required for

cladding pumping, can readily be fabricated during a single deposition run, as opposed to a complex protocol of sequential growths. We have applied this technique to the growth of Er-doped $Y_3Ga_5O_{12}$ (YGG) [11], which is a laser host of particular interest as it possesses emission peaks at 1572 nm and 1651 nm that are aligned with key absorption bands of both carbon dioxide and methane gas, making it an attractive material for use in LIDAR systems [12,13]. In [11] we reported the performance of an Er(1at.%):$Y_3Ga_5O_{12}$ (Er(1%):YGG) waveguide amplifier, with measured internal gains of 0.84 dB cm^{-1} at 1533 nm and 0.44 dB cm^{-1} at 1572 nm seed wavelengths, with an expected internal gain of 0.44 dB cm^{-1} at 1651 nm. Linear propagation losses in this wavelength regime were estimated as being 0.8 dB cm^{-1}.

Here, we demonstrate how it is possible to control the local Ga concentration in an Er(1%):YGG hetero-epitaxial film grown on a <100>-oriented $Y_3Al_5O_{12}$ (YAG) substrate, which maps into a corresponding local change of refractive index within the growing film, and that the degree of Ga inclusion can be precisely controlled via the power level of the CO_2 laser used to heat the substrate during PLD film growth. Finally, we demonstrate the fabrication of an Er(1%):YGG film tailored in a single growth run, to have a specific engineered refractive index profile.

2. Experimental section

2.1 Sample Fabrication

PLD was performed using the experimental setup described in previous work [14], where laser pulses of ~20 ns duration at a repetition rate of 100 Hz, from a 248 nm (UV) KrF Coherent COMPexPro 110 excimer operating at ~ 250 mJ per pulse, were focused into a stainless-steel vacuum chamber to produce a fluence of <1.3 J cm^{-2} on the Er(1%):YGG target surface (see Fig. 1 for schematic of setup). The target was a 5-mm thick, 50-mm diameter, hot-pressed ceramic disc, which was rotated using a DC motor connected to an offset cam in order to maximize the area that could be ablated during a single deposition run. Previously, we have demonstrated compensation of the loss of aluminium during Yb:YAG growth by adding additional Al_2O_3 to the target material [10]. Here, we add an additional 5% Ga_2O_3 to the Er(1%):YGG target to help compensate for potential loss of Ga that routinely occurs during deposition owing to the plume dynamics. PLD was performed under an oxygen atmosphere at a pressure of 2 x 10^{-2} mbar.

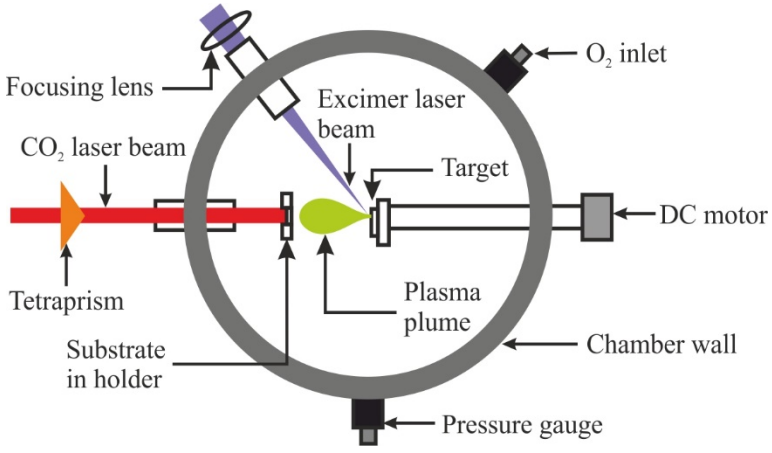

Fig. 1. Schematic of PLD setup.

Ablated material was transferred from the target via a plume to a <100>-orientated 10 mm × 10 mm × 1 mm YAG substrate that had been face-surface polished to optical quality. To enable homogenous heating of the substrates, a CO_2 laser was used (10.6-μm wavelength

(IR), maximum output of 38 W) with a spatial intensity profile that was reconfigured using a tetraprism made of ZnSe [15], generating a top-hat profile on the rear-face surface of the substrate. Such a laser-based technique allows direct heating of the substrate only, thus reducing undesirable heating of the chamber that could otherwise cause desorption of material from the chamber walls and in turn contaminate the growing film [14]. A series of depositions were made in which substrates were heated at a range of CO_2 laser powers, from 6.8 W to 29.5 W, corresponding to substrate temperatures of ~550 ± 25 ^oC to ~1100 ± 25 ^oC, respectively. The corresponding temperatures were estimated via previous calibrations that used a range of metals attached to the substrate to determine the CO_2 power at which each melted [16]. The deposition time for each film growth was 6 min (36000 pulses), leading to a growth of ~2-μm-thick films.

2.2 Measurement

A Rigaku Smartlab diffractometer was used to perform X-ray diffraction (XRD) on the grown films in order to determine their crystal quality. Energy-dispersive X-ray spectroscopy (EDX) was carried out using a scanning electron microscope (SEM) (Zeiss Evo 50) with an Oxford Instruments INCA PentaFETx3 energy dispersive X-ray spectrometer detector. Refractive index measurements of the grown films were performed using a Metricon (2010) m-line prism-coupling system at a wavelength of 633 nm. The thickness of the films was determined using a stylus profiler (KLA Tencor P-16).

3. Results and discussion

3.1 X-ray diffraction analysis

Normalized XRD measurements for Er(1%):YGG films grown on <100>-oriented 1-cm^2 YAG substrates, are displayed in Fig.2. For the same process conditions, apart from the variation of incident CO_2 laser powers, there is a distinct trend in the resultant 2θ XRD peak position for the (400) planes of the resulting ~2 μm-thick crystal films. The (400) XRD peak for the underlying YAG substrate at $2\theta = 29.76^o$ [17] (indicated by a vertical dashed green line) acts as a calibration marker for the position of the YGG peaks. As shown, each (400) YGG peak in the spectra falls below the peak database value at 29.06^o [18], indicated by a black dashed line in the figure. Although there is a 1% substitution of erbium atoms for the yttrium atoms in the crystal lattice, it is expected that this would only shift the (400) 2θ peak position by $+0.02^o$ from the documented pure YGG value, and so we use the latter as the point of reference for the grown films. All of the plots have been normalized to a common film peak height of 1 for ease of comparison. There is no discernable (400) YGG-film peak for a CO_2 laser power of 6.8 W, and the XRD spectrum appears as a horizontal line along the x-axis, since amorphous growth occurs when the substrate temperature is too low to produce any crystalline phase growth.

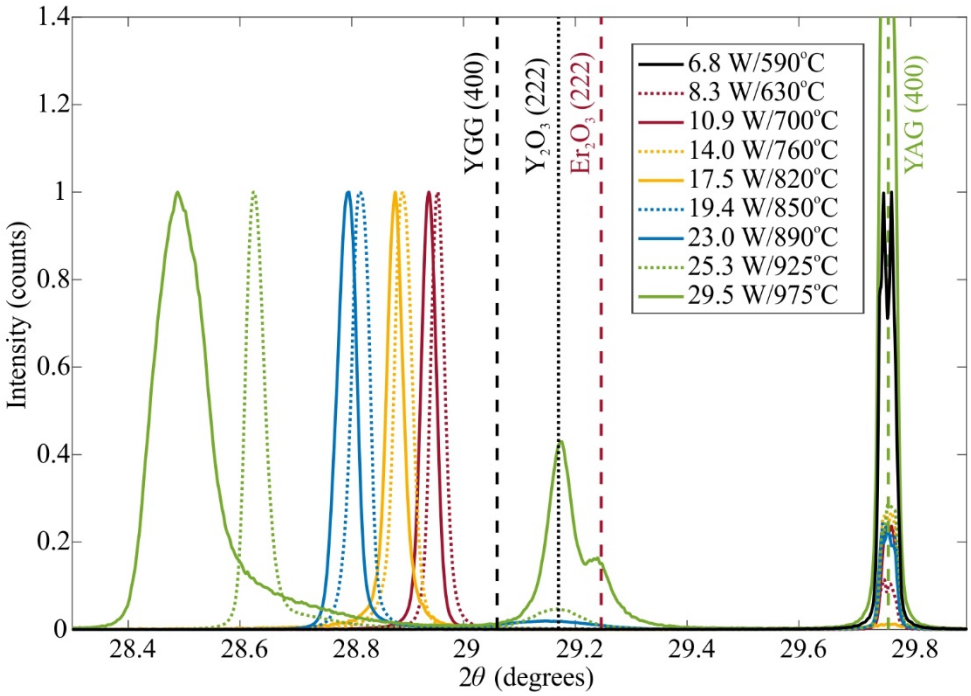

Fig. 2. XRD spectra from Er(1%):YGG films grown at different substrate-heating CO_2 laser powers. The data have been normalized to 1 for ease of viewing. The vertical dashed black line corresponds to the 2θ database value for YGG (400), the vertical dotted black line corresponds to the 2θ database value for Y_2O_3 (222), the dashed red line corresponds to the 2θ database value for Er_2O_3 (222), and the vertical green dashed line corresponds to the 2θ database value for YAG (400).

A plot of the 2θ peak position and full-width at half-maximum (FWHM) of the (400) YGG-film XRD spectra peaks, shown in Fig. 2 as a function of CO_2 laser power, is displayed in Fig. 3. The FHWM of the peaks also reduces with decreasing substrate heating power, indicating that the crystal quality improves with decreasing substrate temperature until falling below the threshold for crystalline growth near 8.3 W CO_2 laser power. It is seen that the narrowest peak FWHM (for growth at 8.3 W) is $<0.03^o$ for its 2θ value, less than the measured bulk YAG substrate FWHM value of 0.03^o hence indicating an excellent degree of crystallinity. At the higher deposition temperatures (CO_2 laser power of 23.0 W and above), there is a low-intensity peak evident at a 2θ value of $\sim 29.17^o$, which is likely due to (222) Y_2O_3 growth (indicated by a black dotted line at a database value of $2\theta = 29.17^o$) [19]. The formation of this yttrium oxide at the highest CO_2 laser powers, suggests that the increasing gallium deficiency at the highest growth temperatures leads to competitive growth of completely Ga-absent Y_2O_3, which is present as a minority constituent within the overall YGG matrix. In addition, also evident at the highest substrate-heating CO_2 laser power is the formation of Er_2O_3 (indicated by a red dashed line at a database value of $2\theta = 29.25^o$) [20], which also likely occurs as a result of gallium deficiency.

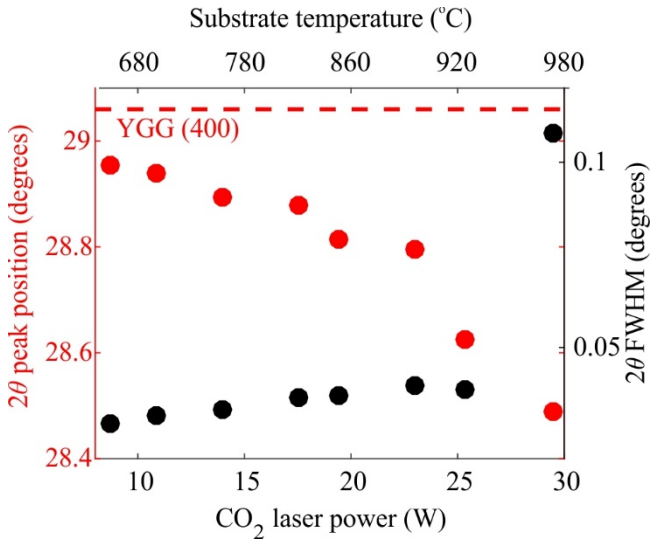

Fig. 3. 2θ FWHM (black dots) and 2θ peak position (red dots) of the (400) YGG-film peak from Er(1%):YGG films grown as a function of substrate-heating CO_2 laser power. Approximate substrate temperatures are quoted on the upper axis. The instrument errors fall within the size of the data points shown. Horizontal dashed red line indicates the 2θ peak position of YGG (400) at 29.06°.

3.2 Energy dispersive X-ray analysis

EDX was used to confirm that the growth of the yttrium oxide was due to a decrease in gallium concentration within the film. The EDX data for the ratio of yttrium to gallium atom concentration, as a function of substrate-heating CO_2 laser power, is displayed in Fig. 4. The plot shows a clear correlation between a CO_2 laser power increase and a gallium concentration decrease, while the relative yttrium concentration increases with increasing CO_2 laser power. Indeed, the increasing concentration of yttrium atoms at a substrate-heating CO_2 laser power of 23.0 W and above, provides good evidence for the observed growth of (222) Y_2O_3 observed in the XRD spectra shown in Fig. 2.

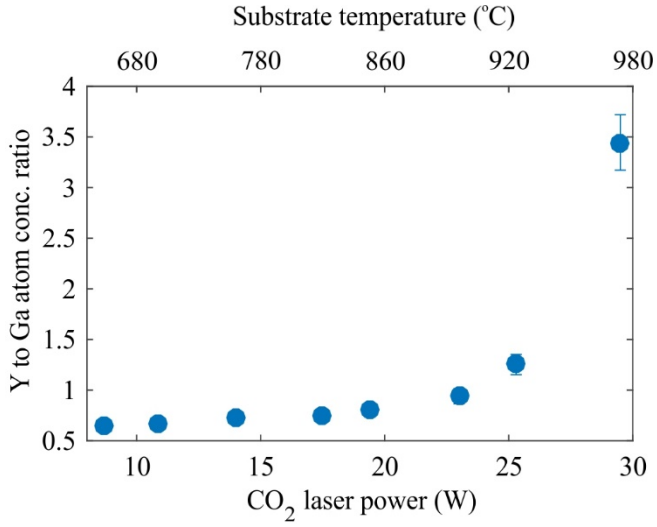

Fig. 4. Ratio of Y atom concentration to Ga atom concentration as a function of substrate-heating CO_2 laser power. Approximate substrate temperatures are quoted on the upper axis.

3.3 Refractive index analysis

Refractive index measurements of the films, taken using a Metricon prism-coupling system, are displayed in Fig. 5 as a function of substrate-heating CO_2 laser power. Data points for the lowest CO_2 laser power of 6.8 W and the two highest CO_2 laser powers of 25 W and 25.9 W were unattainable due to the large number of particulates present in the films, occurring due to amorphous growth at low temperature and highly textured growth of Y_2O_3 and Er_2O_3 at high substrate temperature. It is evident from the plots in Fig. 4 and Fig. 5, that as the CO_2 laser power is increased and the Ga concentration in the grown films decreases, the refractive index of the films shows a corresponding decrease, which is a trend consistent with the refractive index for Y_2O_3 (1.9248 @ 633 nm) [21] being lower than the refractive index of $Y_3Ga_5O_{12}$ (1.9363 @ 633 nm) [22].

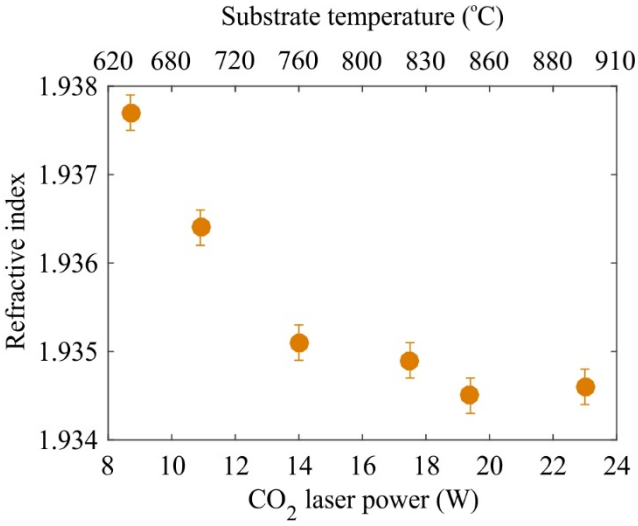

Fig. 5. Refractive index as a function of substrate-heating CO_2 laser power. Approximate substrate temperatures are quoted on the upper axis.

The results demonstrate that a change of CO_2 laser power of 14 W can lead to a change in refractive index of 0.003, and thus, the refractive index of the grown films can easily be controlled by judicious variation of the temperature of the substrate during PLD.

3.4 Bespoke refractive index profile waveguide

As a proof-of-principle, in order to demonstrate the ability to vary the refractive index during deposition and develop a tailored refractive index profile in a single growth run, a waveguide consisting of five ~1.6-μm-thick layers of alternating refractive indices was grown. The design was based on refractive index measurements documented in the previous section. Following deposition, the opposing end facets of the sample were lapped and then parallel polished to yield a waveguide length of 9 mm. An SEM image of the end-facet of the grown waveguide, taken using the secondary-electron detector, is shown in Fig. 6, which also shows the annotated substrate-heating CO_2 laser power profile used during deposition. Although the contrast is poor in this image, which derives from a mere 10 % difference in the Y/Ga ratio, it is evident that we are able to grow discreet refractive-index-defined layers of the desired thickness.

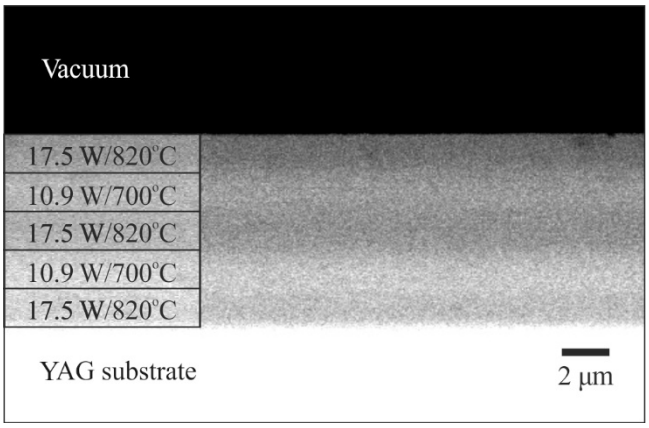

Fig. 6. SEM secondary-electron image of layered film with annotation of corresponding substrate-heating CO_2 laser power profile of substrate during deposition of Er(1%):YGG layers. Approximate substrate temperatures are also included in the annotation.

In order to check that the refractive index of each layer was maintained during the single growth run, the mode characteristics of the waveguide were examined using the Metricon setup, by measuring the effective refractive index for the 17 modes supported by the waveguide structure at 633 nm. Figure 7 shows the measured effective refractive index value of the first 17 modes (red crosses) along with the modelled effective refractive index for the five layer structure (blue circles). Using the single-layer refractive-index data presented in Fig. 5, the modes for the structure shown in Fig. 6 (with equal-thickness layers that combined to a total guiding structure of 8 microns) were calculated by using a finite difference method [23]. This matrix analysis method calculates the effective permittivity of eigenmodes, which are greater than the substrate permittivity, and thus the corresponding guided-mode intensity profiles.

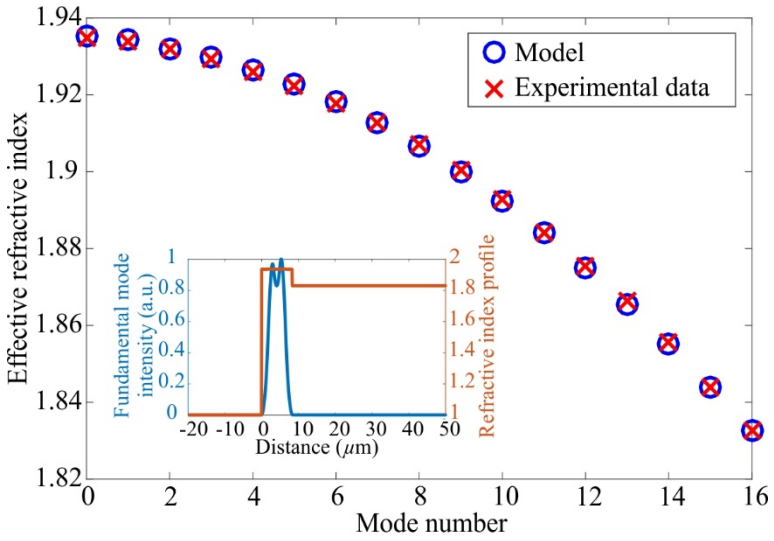

Fig. 7. Effective refractive index measurements for the first 17 modes (red crosses), with modelled refractive index (blue circles), for the five layered film. The error bars for the experimental data fall within the size of the data points shown. Inset: calculated fundamental mode profile, with respect to the refractive index profile of the waveguide structure.

It is evident from the plots that the experimental data matches well with the theory, clearly demonstrating the ability to tailor the optical properties via specific control of the refractive index of a film during a single growth run. Thus paving the way for waveguides with much more elaborate refractive index profiles that allow the potential for bespoke modal control.

4. Conclusion

In summary, we have described the growth of high-quality thin films of Er(1%):YGG on a <100>-orientated YAG substrate via PLD. We have shown how the gallium concentration and in turn the refractive index of the resulting films can be dynamically controlled via the temperature of the substrate onto which the films are grown. Using this technique, we have demonstrated the fabrication of a Er(1%):YGG film with a bespoke refractive index profile on a <100>-orientated YAG substrate grown by PLD in a single growth run. Our results demonstrate the ability to use PLD to engineer thin films for bespoke waveguide designs.

Funding

The authors acknowledge the support of EPSRC (Engineering and Physical Sciences Research Council) through grant numbers EP/L021390/1, EP/N018281/1 and EP/J008052/1, as well as NASA contract GSFC NNG15HQ01C.

Acknowledgements

JAG-J acknowledges support from Dr. Mark Light, School of Chemistry, University of Southampton, for assistance with XRD techniques and Neil Sessions, Optoelectronics Research Centre, University of Southampton, for assistance with EDX. The authors also thank Jake Prentice for discussions concerning the results and Ping Hua for technical assistance. The data for this paper can be found at DOI: 10.5258/SOTON/D0121